New scientific evidence for the history and occupants of Tomb I ("Tomb of Persephone") in the Great Tumulus at Vergina

SUPPLEMENTARY MATERIAL

Contents

S1. A brief summary of the literature regarding the identities of Tomb II and III

S1.1. Tomb II ("The Tomb of Philip")

It is a double-chamber vaulted tomb found untouched by grave robbers bringing up a wealth of valuable finds. In the main chamber among other precious objects a marble sarcophagus was found. Inside was a golden larnax, decorated on top with the famous "starburst" motif with 16 rays, and contained the cremated bones of a male (Andronikos, 1984). In the antechamber another golden larnax, decorated with the "starburst" motif but with 12 rays was also found inside a marble sarcophagus, and contained the cremated bones of a female. After studying the finds Andronikos concluded that this tomb belonged to Philip II (383/2-336 BC), father of Alexander the Great, and one of his wives (Andronikos, 1984). Hence, it was commonly referred to as the "Tomb of Philip II". This conclusion was also supported by N. Hammond (Hammond, 1991, 1982). There were alternative suggestions soon after the discovery for the identities for the male in the main chamber such as Philip III (Arrhidaeus), the son of Philip II and half-brother of Alexander the Great, and his wife Adea-Euridice in the antechamber (Adams, 1980; Lehmann, 1980). The cremains have been studied in the past with several authors supporting the Philp II identity (Musgrave et al., 2010; Musgrave, 1985; Prag, 1990; Xirotiris and Langenscheidt, 1981) and others suggesting the alternative identity of Philip III and Adea-Euridice (Bartsiokas, 2000; Borza, 1987; Gill, 2008), the latter suggestions were either not exclusively osteological or not at all, but based on interpretations of the non-osseous finds. Regarding the skeletal remains as such, much of the controversy focused on whether there was a damage on the facial bones of the male in the main chamber, which according to historical records Philip II had suffered from an injury to his right eye (Riginos, 1994) by an arrow in a city siege, and whether this lesion is conclusive evidence for the identity of Philip II (Bartsiokas, 2000; Musgrave et al., 2010; Riginos, 1994). The identities issue has caused endless debates among archaeologists and historians (Grant, 2019; Hall, 2014; Hatzopoulos, 2008; Lane Fox, 1980; Saatsoglou-Paliadeli, 2011) to name just a few.

A more scrutinized anthropological examination to create a database (Antikas and Wynn-Antikas, 2016) suggested that although there is no evidence of a lesion in the eyes, the cremains of the male, with an age at death estimated to 45±4 years, point to Philip II and the cremains of the female with an age at death estimated to 32±2 points most likely to a Scythian princess, an unrecorded wife of Philip II. Adea Eurydice, the wife of Philip III (Arrhidaeus) was excluded due to the determination of a much higher age for the cremains of the female in the antechamber, whereas Adea died at a much younger age, circa 20 years old. Cleopatra, Philip's last wife must also be excluded as she also died very young. Alternative suggestions for the female may be Meda, Philip's Thracian wife (Hammond, 1991; Hatzopoulos, 2008; Kottaridi, 2020) or Cynnane the daughter of Philip II by his Illyrian wife Audata (Grant, 2019).

The debate has also turned to the identities of the inhumed remains of Tomb I ("The Tomb of Persephone"), whose occupants' identities may indirectly support or dispute suggestions for the occupants of Tomb II.

S1.2. Tomb III ("The Tomb of the Prince")

This tomb contained the cremated and quite fragmented remains of a youth in a silver hydria (Andronikos, 1984). Osteological examination indicated they belonged to an adolescent in the age range 13-16 (Musgrave, 1991; Xirotiris and Langenscheidt, 1981), later focused to 13-15 and it was most likely male (Levesque, 2017; Musgrave, 1991).
Much debate has been voiced regarding the identity of the adolescent interred in this tomb. Early on both N. Hammond and P. Green (Green, 1982; Hammond, 1991, 1982) suggested Alexander IV (323-310/309 BC), the son of Alexander the Great by his Bactrian (or perhaps Sogdian) wife Roxane, who was King for some time before being assassinated by Cassander between 311 and 309 BC (Grant, 2019). Andronikos preferred to maintain a reservation on their suggestion (Andronikos, 1984). Later authors aligned with the identity of Alexander IV (Bartsiokas and Carney, 2008; Borza, 1987; Borza and Palagia, 2007). Some, however, were more cautious or denied the royal character of the Tombs (Faklaris, 1994; Hall, 2014; Palagia, 2017).

The tomb is dated to the end of the 4th century BC (Borza and Palagia, 2007; Gill, 2008). Andronikos (1984) dates this tomb not later than 315-310 BC. A study of papyri fragments found in the tomb revealed that the lunate "C" letter was used replacing the earlier "Σ" (Janko, 2018). This transition, according to Janko, occurred by c. 310 BC hence dating the burial in Tomb III after that date. Grant (2019) suggested that if this tomb belonged to Alexander IV, it could not have been constructed before the death of Cassander (297 BC), who ordered the murder of Alexander IV, and probably not even before his sons who ruled until 294 BC. In any case, the named identity is speculative and would need more investigation to be confirmed.

S2. Ancient DNA analysis

Twenty-four skeletal samples from Tomb I in the Great Tumulus at Vergina were selected for ancient DNA analysis with the aim to determine the biological sex of the individuals. The samples were analyzed at the Manchester Institute of Biotechnology (MIB), University of Manchester, and at the Globe Institute, University of Copenhagen. Both datasets were then analyzed together at the Globe Institute. All the analyses were carried out in accordance with a stringent ancient DNA laboratory procedure, and were conducted in physically isolated, specialised laboratories at MIB and the Globe Institute, equipped with UV lamps that were irradiating the rooms at all times when not in use. Work benches, equipment and consumables were routinely cleaned with 3% bleach and 70% ethanol. All utensils and equipment were further subjected to UV irradiation for 2x5 minutes before and after each procedure. All lab work was performed wearing disposable forensic coveralls, hair nets, protective masks and goggles, gloves and shoe covers, to minimize the risk of contamination with modern DNA. The reagents were prepared with ultraclean water in DNAse- and RNAse-free tubes. Bone samples were processed in batches of 4-8 samples. To further monitor cross-contamination, extraction blanks (full extraction procedure without any starting bone material), and PCR negative controls (PCR setup with ultrapure water rather than bone extract), were included in a ratio of two blanks per four samples.
DNA extractions were performed using 100-200 mg of bone powder following established protocols (Rohland and Hofreiter 2007) including a 10 min “pre-digestion” step (Damgaard et al., 2015). The DNA extracts were then built into Illumina sequencing libraries using two different library preparation protocols. The libraries built in Manchester were built using a double-stranded library preparation protocol (Meyer and Kircher 2010) with minor modifications (González Fortes and Paijmans, 2019). The libraries built in Copenhagen were built using a simplified, single-tube double stranded protocol (Carøe et al., 2018) and a single-stranded protocol (Kapp et al. 2021). All libraries were amplified and indexed using a dual-indexing approach to avoid inaccuracies in multiplex sequencing (Kircher et al., 2012). The optimal number of PCR cycles was determined with qPCR and negative controls were included throughout to monitor for contamination. The libraries were quantified with an Agilent 5200 Fragment Analyzer, pooled in equimolar amounts, and sequenced on an Illumina HiSeq 2500 platform.

Sequencing data was processed using the nf-core/eager pipeline v2.4.3 (Fellows Yates et al., 2021). Adapters were trimmed with AdapterRemoval-2.1.3 (Schubert et al., 2016) using parameters optimized for degraded samples. Read alignment was performed with bwa-0.7.10 (Li and Durbin, 2009) against the human reference genomes, GRCh37 and GRCh38 with the seed function to reduce potential mapping biases due to the 5’ terminal substitutions in the ancient DNA reads (Schubert et al., 2012). Further downstream processing included bedtools v2.26.0 (Quinlan and Hall, 2010) to process the non-collapsed reads and samtools 1.3.1 (Li et al., 2009) to extract the mapped reads. Duplicate reads were removed with PicardTools-1.127 (http://broadinstitute.github.io/picard). Ancient DNA damage patterns were assessed using DamageProfiler v1.1 (Neukamm et al., 2021). Contamination estimates were performed using hapCon (Huang and Ringbauer, 2022). Sex determination was carried out using three different methods including Ry_compute

(Skoglund et al., 2013), SexDetErrmine (Lamnidis et al., 2018), and BeXY (Caduff et al., 2024). For detailed DNA sexing results (see Supplementary 2, Table S2.1, sexing results).

S3. Osteological and Odontological Observations

S3.1. Male bones (listed in anatomical order)

Maxilla-A (samples DEM-3233, 3256) and Mandible A (samples DEM-3235, 3255) (Fig. 7, 8):
Teeth found present in the maxilla's right side: Incisors 1, 2, canine, premolars 1, 2, molars 1, 2, 3. Left side: Incisors 1, 2, canine, premolars 1, 2. Three teeth from the left side were found separate (Fig. 7) but articulated: Molars 1, 2, 3. Teeth found present in the mandible's right side: Canine, premolars 1, 2 molars 1, 2 and 3. Left side: canine, premolars 1, 2 molars 1, 2 and 3. Based on the degree of attrition on molars 1, 2 and 3 from each side of the maxilla and mandible using the schemes of (Brothwell, 1981; Miles, 1962) an age of **25-35** years was estimated for this individual. These teeth, after they erupt into the mouth, wear down in a systematic fashion and continue as an individual ages. This on-going process can vary between individuals and populations due to diet, mastication habits, tooth grinding and other factors; therefore, it is best to use an attrition scheme that is as closely related as possible to the population under study. There is no scheme for ancient Macedonians, so we used methodologies that are closer geographically and chronologically to the Tomb I bones. The Miles scheme is based on an Anglo-Saxon population from England and dated from 700 to 900 AD. Miles found that the rate of wear for this population was similar to that of ancient Greeks (Philippas, 1952). The Brothwell scheme was based on a group of pre-Mediaeval (pre-401 AD) English skulls and is considered the most widely used today to help determine age at death of different populations from different eras (Aldossary et al., 2018). This age estimate, 25-35 years, is in full agreement with Musgrave's estimate (Musgrave, 1985), based on Brothwell's (1981) scheme, but in disagreement with Bartsiokas et al (2015) who gave an age estimate centered around 45 years. That very high estimate is based on a scheme derived from a Late Woodland (900-1650 AD) Native American population from Libben, Ohio, USA (Lovejoy, 1985) found to be similar to that of Australian Aborigines (Murphy, 1959); a scheme rather inappropriate for the European Continent populations.

Right humerus (DEM-3239) (Fig. S3.1): The proximal end is missing but some dimensions could be taken of its distal end to compare with the left humerus (Bass, 1995):
1. Epicondylar width: 59mm
2. Articular width: 44.5mm

Left humerus (Fig. S3.1): When excavated was in two pieces but articulates at the mid-diaphysis to make a complete bone.
Dimensions taken that are helpful to determine sex (Bass, 1995):
1. Maximum length: 316mm
2. Vertical diameter of the head: 49mm
3. Epicondylar width 58.7mm
4. Articular width: 44.8mm

The vertical diameter of the head is considered the most useful to determine sex with this bone. A formula based on a study by (Stewart, 1979) stated that the vertical dimension of the head ≤ 43mm is female, 44-46mm sex is indeterminate and over 47mm is

male. The diameter of the left humerus head is 49 mm, which puts it clearly in the male range. The humeri distal articular dimensions are practically the same (Fig. S3.2).

Right (in-situ) femur (DEM-3242) and left in-situ femur (Fig. S3.3): The right bone was sampled because it was found incomplete with the proximal and distal ends separate and fragmented (Fig. S3.3A). Due to its fragmentary nature, it was not possible to take its dimensions with any accuracy (Table 1). However, the left bone was found intact (Fig. S3.3B) and gave dimensions that are helpful for sex and height estimation, these are:

1. Maximum length: 439mm
2. Mid shaft anterior-posterior diameter: 27.7mm
3. Mid shaft medio-lateral diameter: 25.5mm
4. Mid shaft circumference: 100mm
5. Maximum head diameter: 51.1mm

According to a study on Mediterranean populations of the late Roman period from Spain (Safont et al., 2000), the mid-shaft circumference of the femur for males is 89.1 ± 5.47 (1sd) and for females 78.55 ± 5.16 (1sd) with a success rate over 82-92% including several other sites and periods in Spain. As seen from the circumference of the left femur (index 4), the value of 100 mm is above even 3 standard deviations from the mean female value found by Safont et al (2000). Furthermore, the femoral head diameter in males has been found to be >47.5 mm (Bass, 1995), which brings the value of 51.1 mm for the left femur (index 5) also in the male range. Thus, this bone belongs clearly to a male which also agrees with the DNA assignment. A stature, using the left femur, was calculated at 167.4 ± 3.94 cm using a formula for white males (Trotter and Gleser, 1952). It is assumed the right femur, if intact, would give similar dimensions since these bones belong to the same person as indicated by their in-situ position in the tomb.

The left femur head shows the persistence of an epiphyseal line (Fig. S3.4). A study by Belcastro et al (Belcastro et al., 2019) on the persistence of an epiphyseal line in the appendicular skeleton of 981 adult male and female skeletons from a 19^{th}-20^{th} century Italian and Portuguese skeletal collections, assigned 4 degrees of fusion for the femoral head with 0 being none and 4 complete. The femoral head discussed here shows Degree 3. It is characterized by complete union with persistence of the epiphyseal line. This line is visible due to the persistence of a "scar". This scar can take the shape of a porous line or a groove. Those researchers found that Degree 3 can be considered a good marker of a young adult aged less than 34 years.

Right (in-situ) tibia and left (in-situ) tibia (DEM 3243) (Figs. S3.5): The proximal end of the left tibia was damaged. The right one was in two pieces when it was excavated, but articulated to make an intact bone. Some dimensions could be taken and were helpful for sex and stature estimation, they are:

1. Maximum length: 357 mm
2. Anterior-posterior diameter at the nutrient foramen: 36.4 mm
3. Medio-lateral diameter at the nutrient foramen: 22.4 mm
4. Circumference of the diaphysis at the level of the nutrient foramen: 96.7 mm

In the same study (Safont et al., 2000) mentioned above, the authors conclude that the circumference of the tibia diaphysis at the level of the nutrient foramen is one of the best discriminators for sexual dimorphism. They found that this value for 32 males was: 95.31 ± 5.45 mm (1sd) and for 45 females 79.89 ± 4.96 mm (1sd). The circumference of the diaphysis of the in-situ left tibia is 96.7 mm, a value which is above even 3 standard deviations from the mean value of the females and hence places it clearly in the **male** range and agrees with the DNA assignment. Stature was calculated with the left tibia at 168.5 ± 3.37 cm for a white male (Trotter and Gleser, 1952). This stature is similar to the one calculated from the left femur mentioned previously. Therefore, due to the fact that both these sets of leg bones (femora and tibiae) are DNA sexed **male** and have a similar morphology and size, we believe they belong to the same person. Using both the femur and tibia, a more accurate stature was calculated at 166.8 ± 2.99 cm, again following the methodology of Trotter and Gleser (1952). That value is in general agreement with Musgrave's (1985) calculation for this male based on the length of the left femur (165.18 ± 3.27 cm) and also with Bartsiokas et al's calculations (Bartsiokas et al., 2015), circa 165 cm, with the difference being the latter paper wrongly concluded this individual was female.

S3.2. Maxilla-B (female)

Maxilla B (Fig. 9) (DEM-3237): This bone and teeth are seen in Cluster Γ on the excavation drawing (Fig. 6). It belonged to a female confirmed by DNA analysis. Teeth found present and in their alveoli are: Right side: canine, premolars 1, 2, molar 1 and molar 3. Left side: Lateral incisor and premolar 1. Four teeth from the left side were found separate (Fig. 9): Premolar 2, molars, 1, 2 and 3. Left molar 1 with attached bone (DEM-3237) was sampled for DNA and other tests listed on Table 1. Age estimation was through: 1) dental attrition of the extant molars, 2) root closure timing and 3) suture obliteration of the maxilla. An age range of 18-25 years at death was determined using methods 1 and 2 and 20-24 using method 3. Regarding dental attrition, the (Brothwell, 1981; Miles, 1962) schemes also used for the male maxilla/mandible A were found to be the most appropriate schemes to apply for the same reasons mentioned previously. An age range of 18-25 was estimated using left molars 1, 2 and 3. Right molar 2 is not present so the left side was preferred, although right molars 1 and 3 were used to compare with their counterparts on the left. The upper end of the age range was placed at 25 because there is no dentin exposed on molars 3 which indicate they are from a young adult. The lower end of the age range was estimated through the closure timing of the apical ends of the root of left molar 3 (Fig. 9) (Mincer et al., 1993). That study found in maxilla belonging to females <25 years of age with the apical ends of the root closed on molar 3 there is an 89.6% probability they are ≥18 years of age.
A method used to age human male and female skeletons at age of death using the hard palate of their maxilla was developed by (Mann et al., 1987) and then revised by (Mann et al., 1991). This method divides the maxilla's sutures into four parts: the incisive, anterior median palatine, transverse palatine and posterior median palatine. These sutures follow a general pattern of closure as an individual ages with the incisive being the first to close. Which means if that suture is completely closed you would then go to the next suture to estimate age at death and so on. A study by (Apostolidou et al., 2011) of 270 (150 males and 120 females) Greek skeletons of known sex and age at death who lived mainly in the 2nd half of the 20th century were studied using the revised Mann study found that 84% of the

females were aged correctly. Maxilla B's sutures were examined to see where they were in the process of closing. The incisive suture was not completely obliterated (Fig. S3.6) which would indicate an age for this female between 20-24 years old. That age range generally corresponds to the range given for the other age indicators for her teeth, namely, the dental attrition and root closure timing.

S3.3. Unsided femur fragment

Unsided femur diaphysis (DEM-3128): This femur fragment is of gracile morphology compared with the femora of the ISM. It is an unsided fragment of approximately the mid diaphysis of the bone and has some erosion on its cortical surface, so a full set of measurements were not possible. However, we were able to measure approximately its circumference at a nutrient foramen and close to mid-diaphysis which gave 78 mm with an estimated maximum of 79mm. This value is within the female range of Roman period skeletons from Spain (78.55 ± 5.16, 1sd) and below or at the limit of even two deviations from the mean value for males (89.1 ± 5.47, 1sd) of Roman period skeletons from Spain, found in the same study (Safont et al., 2000). This fragment was found on the floor, and appears in the 1977 excavation photo (Fig. 5). Its position was approximately in the middle of the tomb, separate from the three bone clusters. It could not be reliably sexed by DNA but its gracile morphology along with its mid-shaft dimension suggest it belongs to a female.

S3.4. The fused leg bones with the hole

Stella Drougou who excavated the entire fill of the tomb in 1977, writes in the logbook: "the lengths of the biggest bones are 43 cm and 38 cm". These obviously correspond to the in-situ femora and tibia (Fig. 5) fully studied and analyzed in this work. They correspond to a male with stature of about 166-167 cm calculated both by us and Musgrave (1985). In addition, P. Faklaris who removed the bones from Tomb I the following year (1978), considered they belonged to one skeleton (since there were only two femora, left and right, and two tibiae, left and right) and he describes the bones he found in the three different Clusters.

Therefore, namely the archaeologists S. Drougou, P. Faklaris and A. Kottaridi, who were present at the excavation of this tomb and made a drawing of all the floor bones before their removal in 1978 (Fig. 6), including Andronikos himself, never saw, photographed, described or recorded in photos and drawings this "gigantic" fused femur-tibia bones with the hole (Fig. S3.13, Fig. S3.14). Certainly, there is no way that such a unique pair would have gone unnoticed by the excavators S. Drougou, P. Faklaris, and A. Kottaridi even more so since they took notice and recorded small bones on the floor and within the fill, and by Andronikos who never mentioned such a pair. It is impossible that it could have gone unnoticed also by Musgrave who examined the bones at the Archaeological Museum of Thessaloniki (AMTh). Musgrave, in particular reported that the Tomb I bones were all contained in one box, with the limb bones wrapped separately in tissue and the smaller ones in polythene bags (Musgrave, 1984). Musgrave found in the box only two femora, left and right, and two tibiae left and right belonging to the same man and says: "he was well-built, but not very tall about 1.65-1.66 m probably in his prime of life" (Musgrave, 1985, 1984). He never observed or reported on this additional large left femur and tibia fused together with

the hole. Additionally, Professor N. Xirotiris, who took the bones to Komotini for further study, stated in an interview to the Greek newspaper *Kathimerini* (Xirotiris, 2015) following the publication by Bartsiokas et al (2015), that this fused pair of huge leg bones with the hole never existed in the original collection of bones from Tomb I that was given to him in a box by Professor M. Andronikos as he said, but it must be coming from another excavation from Crete, Epirus, Chalcidice etc., bones of which existed in the Anthropological Laboratory of the Democritus University of Thrace.

Furthermore, the outer or cortical surfaces of this pair of bones shows a different erosion morphology. They are darker in color, exhibit plant root imprints, pitting and differential surface erosion (Fig. 10 main text and S3.14), features not seen on the bones found and recorded inside Tomb I. The difference is also apparent on a photo of the bones taken in 2012 by Mr. Matthaios Koutsoumanis, Head of Department of Classical Antiquities and Museums of the Rodopi Ephorate of Antiquities at Komotini, who spotted the Tomb I bones on a visit to the Laboratory of Anthropology at the Democritus University of Thrace (Fig. S3.15). In contrast, the rest of the Tomb I bones are almost white, most probably because of the rich in carbonates soil from the limestone walls of the tomb. The fused leg bones were most probably buried in a totally different soil environment; such as one that would be expected in a shallow grave more vulnerable to surface climatic changes and plant activity (Surabian, 2012). Finally, the long bones from Tomb I that were transferred from Vergina to Komotini in the late 1980s, were wrapped separately in newspaper bearing the date 1985 with the smaller ones wrapped in white tissue and placed in polythene bags as Musgrave described it when he first examined these bones at the AMTh in 1984. Contrary to that, this pair (the two long bones on the upper left corner of the picture, Fig. S3.15) are not wrapped in tissue or newspaper.

Table S3.1. List of Tomb I bones "on the floor" collected in the 1978 excavation (Fig. 6, main text).

Bone (number of fragments)	**Analysis number***
Maxilla-A with teeth	DEM-3233, 3410, 3256
Mandible-A with teeth	DEM-3235, 3255,
Maxilla-B with teeth	DEM-3237
Clavicle, scapula, humerus head fragment (23)	
Left humerus	
Right humerus, left radius, right ulna	DEM-3239, 3248
Vertebra (8 and many small fragments)	
Ribs (37)	
Innominate (Pelvis) (ten)	DEM-3412
Coccyx and sacrum fragments (2)	
Hand and foot metacarpals, metatarsals and phalanges (31)	DEM-3238, 3274, 3240, 3241
Hand and foot carpals/tarsals (16)	
Right and left talus, right and left calcaneus	
Cranial fragments (31)	
Cranial fragments (4), including a left petrous, sampled and left temporal bone fragment with mastoid process	DEM-3236
Cranial fragments (4), including right zygomatic/frontal bone, sampled	DEM-3244
Cranial fragments (9), including a right petrous, sampled	DEM-3246
Left femur	
Right femur	DEM-3242
Right tibia and fibula	DEM-3413
Left tibia and fibula	DEM-3243
Perinate fragments (20), including one left petrous and one sphenoid both sampled	DEM-3245, DEM-3273
Animal, *capra/ovis* metacarpal (found outside Tomb I)	DEM-3411
Pyre remains with charcoal and animal bones (found outside Tomb I)	DEM-2719

Note: * DEM numbers correspond to samples taken from specific bones in each group (for details see main text, Tables 1 and 2).

Table S3.2 Bones "in the Fill" from the 1977 excavation, stored at Vergina*

Inv. no.**	Bone	Dimensions (mm)/Weight (g)	Approx. Age, Sex
Adults			
A2b (DEM-3134)	Proximal hand phalange, 5th finger	Length 32.4/1.1	Adult, unsexed
A2c	Intermediate hand phalange, 2nd finger	Length 26.8/1.1	Adult, unsexed
A2d	Proximal foot phalange, 1st toe	Length 29.5/1.3	Adult, unsexed
A2e1	Vertebral body fr.	27.5x23.9/1.4	Adult, unsexed
A2e2	Vertebral body fr.	24.4x15.6/0.6	Adult, unsexed
A2g (DEM-3133)	Rib body fr.	Length 67.5/2.8	Adult, unsexed
A2h	Rib body fr.	Length 40.9/1.3	Adult, unsexed
A2i	Rib body fr.	Length 43.2/1.2	Adult, unsexed
A2j	Rib body fr.	Length 45.3/0.7	Adult, unsexed
A2k	Sternal end of rib fr.	Length 30.4/0.5	Adult, unsexed
C2l (DEM-3128)	Femur diaphysis fr. (unsided)	Length 205.0/63.6 Circumference at mid-diaphysis: 78-79 mm	Adult, probably female
C2m	Right temporal fr.	Length 83.7/31.2	Adult, unsexed
C2n	Left scapula fr. Includes middle and inferior portion of the glenoid cavity and infraglenoid tubercle	Length 87.6/8.8	Adult, male
C2o (DEM-3127)	Left scapula fr. Includes the coracoid process and superior portion of the glenoid cavity	Length 87.5/9.1 (Full length of glenoid cavity=39 mm	Adult, male (glenoid cavity joins with C2n)
C2p (DEM-3126)	Right metacarpal-1	Length 46.3/3.2	Adult, male
C2q1	Right radius proximal end	Length 83.4/8.8	Adult, male (joins with C2q2 and q3)
C2q2 (DEM-3125)	Right radius diaphysis	Length 123.9/14.2	Adult, male (joins with C2q1 and q3) (Fig. S3.9)
C2q3	Right radius distal end	Length 56.0/4.5	Adult, male (joins with C2q1 and q2)
C2r1	Left ulna proximal end	Length 19.2/6.4	Adult, male (Fig. S3.10)
C2r2	Left ulna diaphysis	Length 195.0/19.4	Adult, male joins with C2r1
C2t	Rib, head	Length 63.0/5.0	Adult, unsexed
Fetus/perinates			
A1	Right humerus fr.	30.5x17.3/0.8	8-10 LM, unsexed
A2	Right ulna fr.	Length 23.7	8-10 LM, unsexed

A3	Left ulna fr.	Length 27.4	8-10 LM, unsexed
A4	Right femur, 2 fr.	Length 81.3/3.5	10 LM, unsexed
A5	Occipital bone	16.8x16.2	10 LM, unsexed
A6	Left zygomatic	18.3x19.1/0.3	10 LM, unsexed
A7	Right zygomatic	17.2x21.3/0.2	8 LM, unsexed
A8	Right zygomatic	15.7x15.4/0.3	8 LM, unsexed
A9	Left petrous	37.5x17.9	10 LM, unsexed
C11 (DEM-3129)	Left petrous	Length 39.2/2.6	10 LM, unsexed
C12 (DEM-3130)	Left petrous	Length 36.8/1.8	8-10 LM, unsexed
C13 (DEM-3131)	Left petrous	Length 39.2/1.6	10 LM, unsexed
C14 DEM-3132)	Left petrous	Length 23.0/0.9	6.5-10 LM, unsexed
C15	Right petrous	Length 38.7/2.9	10 LM, unsexed
C16	Right petrous	Length 35.2/3.5	8-10 LM, unsexed
C17	Right petrous	Length 36.7/1.8	8-10 LM, unsexed
C18	Right body of mandible	Length 50.2/1.0	Perinate
C19	Right body of mandible	Length 47.8/0.9	Perinate
C20	Right body of mandible	Length 48.6/1.2	Perinate
C21	Left body of mandible	Length 48.6/1.2 -	Perinate
Animals			
Inv. no.	**Bone**	**Dimensions (mm)/Weight (g)**	**Species/comments**
AA (DEM-3137)	Tibia-fibula fr.	60.8x23.0/8.6	*Capra/Ovis*, bears traces of butchery marks (Fig. S4.8)
AB	Talus	35.4x22.9/4.6	*Canis*? Shows traces of red painted plaster
AC (DEM-3138)	Humerus fr.	Length 54.8/8.6	*Felis*? Small animal, not ruminant
AD (DEM-3139)	Horn fr.	Length 58.5/13.5	*Capra/Ovis*, bears traces of butchery marks (Fig. S4.8)
AE (DEM-3140)	Tibia fr.	Length 66.6/99.0	*Canis*? Upper limb of medium-sized animal, not ruminant

* The Osteological/Osteometric examination initially performed by Theodore Antikas and Laura Wynn-Antikas in 2014 is updated for this publication.

** The DEM numbers indicate bones that have been sampled and analyzed.

S4. Radiocarbon Dating

S4.1. Detailed collagen extraction of some samples

Thirty-five samples were pretreated for radiocarbon dating. Six samples failed to produce enough collagen for reliable dating. Two of these, the in-situ femur (DEM-3242) and in-situ tibia (DEM-3243), considered particularly important and the amount of sample permitted, were sent to the Department of Human Evolution, Max Planck Institute for Evolutionary Anthropology MPI-EVA, Leipzig for a more detailed collagen extraction procedure (Talamo et al., 2021; Talamo and Richards, 2011).

The samples underwent an 'acid-base-acid' (ABA) sequence designed for decalcification, decontamination, and gelatinization of the bone chunks. This process began with an initial treatment in hydrochloric acid (HCl 0.5M) to dissolve mineral substances and some organic pollutants. Once the CO_2 effervescence ceased, the demineralized samples were rinsed with ultrapure Milli-Q water and then treated with sodium hydroxide (NaOH 0.1M) for 30 minutes at room temperature. Following this, the NaOH was replaced with ultrapure water for an additional rinsing step.

Subsequently, the water in the glass tubes was removed and replaced with HCl 0.5M. The bones were re-acidified for another 15 minutes at room temperature. Using a heater block, the resulting collagen was dissolved and converted into gelatin in acidic water (HCl, pH 3) at 70°C for 20 hours. The obtained gelatin was first filtered with Eeze-filters to remove small particles (>80 μm) and then through an ultrafilter to effectively separate low molecular weight contaminants or degraded proteins (<30 kDa) from larger molecules (>30 kDa). Prior to use, the Eeze filters and ultrafilters were meticulously precleaned to avoid contamination from the filter membranes.

After ultrafiltration, only the >30 kDa fractions were frozen for 24 hours and then freeze-dried for 48 hours. The suitability of the extracts for dating was evaluated based on collagen yield (minimum requirement ~1%) and elemental values (Talamo et al., 2021; van Klinken, 1999). All extracts displayed characteristics of well-preserved collagen (Table 2) and were submitted for dating via accelerator mass spectrometry (AMS) at the Curt-Engelhorn-Center for Archaeometry in Mannheim, Germany (CEZA, lab code: MAMS). At CEZA, the collagen was combusted to CO_2 in an elemental analyzer (EA) and catalytically converted to graphite before measurement on a MICADAS AMS (Kromer et al., 2013).

S4.2. Models used in the statistical analysis

The outlier model used in combination with one-phase Bayesian analysis was of the type: [*Outlier_Model("General",T(5),U(0,4),"t")*], where T(5) defines a student-t distribution with 5 degrees of freedom, U(0,4) is the range of dates to be considered (0-10000 years) and “t” for outliers in the time variable (Bronk Ramsey, 2009). This was in order to check for possible outliers in this phase. The prior outlier value was set to 5%. The output of this analysis is shown in the plots of figures S4.1, S4.2, S4.3, S4.4, S4.5 and Fig. 12 and 13 of the main manuscript.

S4.3. Collagen offset details and correction models

During childhood there is a fast collagen turnover in the bones (new collagen deposited exchanging the old one) and up to about the age of 20 the turnover rate is still relatively fast. After that the turnover slows down and for an adult it is estimated to be 3-4% per year although the variance is large (Hedges et al., 2007; Manolagas, 2000). This would mean for an adult 30 years old, 30-40% would be new collagen and 70-60% older collagen. This may cause an offset in the radiocarbon age which may be increasing with the age at death of the individual. Calculations show that age offsets are expected to be on the order of 10-15 years for the age of individuals between 30-50 years (Bayliss et al., 2013).

In order to test the effect of the collagen offset on the dating of the in-situ bones and apply a certain correction, we used the following models:

In-situ male bones (femur and tibia) collagen offset correction model:
The age at death of this in-situ male is estimated to be 25-35 years as discussed in the osteological and odontological section. Hence, we applied a model that has the following script and run it with the Oxcal v.4.4.4 program:

```
Options()
 {
  Resolution=1;
  ConvergenceData=TRUE;
 };
 Plot()
 {
  Outlier_Model("DEM-3242_3243_Male_25_35",N(-10.9,1.9),0,"t");
  R_Date("DEM-3242,3243", 2318, 18)
  {
   Outlier("Male_25_35",1);
  };
 };
```

The combined radiocarbon date of the two bones (2318 ± 18) was used in the model. A mean collagen offset of 10.9 is considered for this age range at death with an uncertainty of 1.9 taking into account the 10 years spread of the age estimate (25-35). These offset values are taken from the Cambridge University "After the Plaque" Project (Craig Alexander, personal communication).

Female bones offset correction model:
The age at death of the female is estimated to be 18-25 years as discussed in the osteological and odontological section. Females in this age range may exhibit a collagen offset of 8 ± 0.9 years, according to the Cambridge University "After the Plaque" Project (Craig Alexander, personal communication). In this case and using the combined radiocarbon date of the three female bones (2286 ± 14 BP), we applied the same model as above but with different parameters:

```
Options()
 {
  Resolution=1;
  ConvergenceData=TRUE;
 };
 Plot()
 {
  Outlier_Model("All_Female_Floor_18_25",N(-8.4,0.9),0,"t");
  R_Date("All_Female_Floor", 2286, 14)
  {
   Outlier("Female_18_25", 1);
  };
 };
```

S5. Stable isotope analysis for $\delta^{13}C$ and $\delta^{15}N$

The remainder of the collagen from the samples that had produced more than enough for AMS dating plus some additional bone samples were submitted for isotope ratio analysis ($\delta^{13}C$ and $\delta^{15}N$) to Elemtex Ltd at Callington, Cornwall. For extracting the collagen, from the bone, the samples were demineralized in 0.5M HCl in the fridge at circa 4°C until completion and the resulting organic material was solubilized by heating at 60°C in HCL at pH3 for 24 hours before being ultra-filtered to 30kDa. The solution was then freeze dried to give collagen ready for analysis. All collagen samples were analyzed for stable isotopes on an *ANCA SL* elemental analyzer linked to a *Sercon 2020* isotope ratio mass spectrometer. A triplicate analysis was performed for each sample. The mean values of the triplicate results and other details are presented in Table S5.1. The atomic C/N ratio ranges from 2.9 to 3.3, and the carbon and nitrogen percentage yield varied between 16.28–43.14 and 6.01-16.28% respectively. These values all lie within the accepted standards (Ambrose, 1990; Cheung et al., 2012; DeNiro, 1985; Harbeck and Grupe, 2009) suggesting that the collagen in the bones was fairly well preserved.

Table S5.1. Stable isotope results

Sample code	Name	Sex	Mean $\delta^{15}N$	Mean $\delta^{13}C$	C/N	%N	%C
Adult bones							
DEM-3242	In-situ Femur	Male	10.03	-18.63	3.26	14.16	39.60
DEM-3243	In-situ Tibia	Male	10.25	-18.44	3.18	6.01	16.36
DEM-3413	In-situ Fibula	Male	10.38	-18.50	3.14	13.53	36.34
DEM-3239	Right Humerus	Male	10.34	-18.98	3.33	13.16	37.55
DEM-3125	Right Radius	Male	10.26	-18.61	3.15	7.98	22.95
DEM-3126	Metacarpal	Male	9.96	-18.99	3.08	15.98	42.37
DEM-3133	Rib body	n.a.	9.76	-18.87	3.09	16.28	43.14
DEM-3127	Left-scapula	Male	9.61	-19.03	3.10	15.98	42.52
DEM-3274	Metatarsal	n.t.	9.46	-19.30	3.15	9.10	24.53
DEM-3412	Innominate/pelvis	Male	9.81	-19.11	3.22	12.77	35.26
DEM-3134	Hand phalange	Male?	9.56	-19.13	3.18	15.70	42.84
DEM-3128	Unsided femur diaphysis fragment	n.a.	11.61	-18.56	3.10	11.14	29.55
DEM-3246	R-Petrous portion	Female	11.13	-19.25	3.20	8.50	23.34
DEM-3276	Unknown origin fused pair-femur/tibia	Male	10.63	-20.17	3.26	15.28	42.64
Baby bones							
DEM-3130	L-petrous portion, Fetus/perinate	-	9.61	-19.53	3.12	15.60	41.63
DEM-3129	Left petrous portion, Perinate	-	10.10	-19.50	3.11	14.12	36.94
Animal bones							
DEM-3414	*Capra/ovis*, metacarpal		3.96	-20.60	3.12	15.93	42.62
DEM-3137	*Capra/ovis,* tibia/fibula		4.11	-19.99	3.22	13.79	38.02
DEM-3138	Small animal *Leporidae* (hare/rabbit?), humerus		4.90	-21.06	3.13	15.98	42.86
DEM-3411	*Capra/ovis*, metacarpal, from pyre outside the Tomb		7.65	-16.02	3.05	13.25	34.67
DEM-3140	Animal (*canis*,Dog), tibia		8.42	-19.36	3.11	11.36	30.30

S6. Strontium isotope analysis

S6.1. Samples

Small fragments of a few mg of enamel from three human teeth were sampled for strontium isotope analysis. Two tooth enamel samples are from the in-situ male individual (ISM), one tooth from the maxilla-A and another tooth from mandible-A (DEM-3255, 3256). The third enamel sample comes from a tooth from the maxilla-B (DEM-3237), which belongs to The female.

Samples from the otic capsule of petrous bones and the in-situ long bones (femur and tibia) from the ISM were also analyzed. These bone samples were carefully pre-treated with 0.1 N acetic acid (Sillen, 1989, 1986) prior to dissolution to remove potentially present diagenetic carbonates.

In order to establish the baseline of the area, modern samples of water and plants were collected from the archaeological sites of Vergina and Pella. In addition, extracts of ancient soil samples from the archaeological excavations in each site were also analyzed. The modern plant samples were composed of leaves from bushes and trees growing inside the protected archaeological areas. The water samples were collected, in the case of Pella, from ancient wells still carrying water, and in the case of Vergina, from a creek flowing down the hills about one kilometer southwest of the respective archaeological site. In addition, a few bone fragments and tooth enamel from the ancient fauna found inside the fill of Tomb I were also analyzed to complement baseline samples and were leached with 0.1 N acetic acid prior to dissolution.

The following methodological procedures were applied:

S6.2. Sample preparation

The water samples were filtered through 0.45µm syringe filters. 10ml aliquots were pipetted into pre-cleaned Teflon beakers and dried down on a hot plate at 100°C overnight. The soil samples were air dried and gently ground using an agate mortar. A 1M sodium acetate leachate of the soils was chosen to represent the bioavailable Sr. For this, 1g of unreacted soil was weighed into a 15ml test tube. 5ml of a 1M sodium acetate (NH_4NO_3) solution was added to the test tubes, which were then placed in an overhead-shaker for 2h. Subsequently, the samples were left to settle for 1h before being centrifuged. This extraction follows the procedure applied in the Europe-wide soil-based bioavailable strontium isotope survey, which was performed as part of the Geochemical Mapping of Agricultural and Grazing Land Soil (GEMAS) framework program (Hoogewerff et al., 2019). 1ml aliquots of these leachates were used for the Sr isotope analyses. These aliquots were dried down on a hot plate at 100°C.

The plant samples were washed in ultrapure water, then air-dried, and subsequently crushed in an agate mortar. For analysis, 0.1g of the plant material sampled were weighed into pre-cleaned ceramic crucibles. The samples were incinerated in a laboratory muffle furnace at 750°C for 5h. After cooling, the samples were transferred into pre-cleaned Teflon beakers using ~2ml ultra-clean (Milli-Q 18Ohm resistivity) water (MQ) and dried down on a hot plate at 100°C. Next, the samples were digested further on a hotplate at 100°C using 1ml concentrated HNO_3 and then evaporated to dryness again.

Sampling and pre-treatment of bone, tooth enamel and petrous bone sample material followed that described in (Frei et al., 2017, 2015). Sample amounts ranging between 2 and 5 mg were placed into 7ml Savillex Teflon beakers. They were dissolved in 0.5ml of a mixture of concentrated HNO_3 and H_2O_2. Some samples (petrous bones, femur and tibia) were additionally spiked up with an appropriate volume of a highly ^{84}Sr-enriched spike solution which enabled the determination of the Sr concentrations in these samples via isotope dilution scripts. Before ion chromatographic separation of Sr, the samples were dried on a hotplate.

S6.3. Sr separation

The Sr separation procedure was based on the methods described by (Frei and Frei, 2011). 1ml pipette tips were used as disposable extraction columns. They were mounted with a pressed-in filter, pre-cleaned in 6M HCl and charged with 200 µl pre-cleaned SrSpec™ resin (50–100 mesh; Eichrome Inc./Tristchem) conditioned with 3M HNO_3. The dried down water, soil leachates and plant samples were re-dissolved in a few drops of 3M HNO_3 and loaded onto the columns. Next, the matrices were washed out using ~10ml of 3M HNO_3 before Sr was then eluded with ~2ml of MQ. The final solutions were dried down on a hot plate at 100°C.

S6.4. Thermal ionisation mass spectrometry (TIMS)

All the TIMS measurements were performed at the Department of Geoscience and Natural Resource Management (IGN) at the University of Copenhagen using a VG Sector 54 IT mass spectrometer equipped with eight Faraday detectors. 2.5µl of a Ta_2O_5-H_3PO_4-HF activator solution was used to load the samples on previously outgassed 99.98% single Re filaments. The samples were analysed in dynamic multi-collection mode at analysing intensities ≥1V for ^{88}Sr and temperatures between 1300-1350 °C. The NBS 987 Sr standard returned a $^{87}Sr/^{86}Sr$ ratio of 0.710237± 0.00002 (n = 4, 2σ). The measured $^{87}Sr/^{86}Sr$ values of the samples were corrected for the offset relative to the certified NIST SRM 987 value of 0.710245 (Thirlwall, 1991). The within-run precisions (2SE) of the individual runs were as high as 34ppm, but usually values of ≤15ppm were achieved. Procedural Sr blanks were between 20pg and 60pg strontium, with $^{87}Sr/^{86}Sr$ values between 0.7095 and 0.7122. The contribution of blank-related Sr to the overall sample Sr (typically ≥200ng) is insignificant and thus no blank corrections of the measured values were necessary.

S6.5. The geology of Vergina and Pella regions and the baseline values

The Vergina baseline samples exhibit Sr isotope signatures in the range from 0.70986 to 0.70992 (Table S6.1). The ancient site of Vergina is situated on the south-western side of the Thermaikos graben, at the foot of the Pieria Mountains. These are dominated by ophiolites, and descend via Cretaceous limestones and flysch to the alluvial plains. The ancient city was constructed on the lower slopes of the hills and the palace stood on the edge of the plain. The tombs were excavated out of the alluvium – red clays with boulders of serpentinite. Since ophiolithic rocks and Cretaceous limestones are expected to be characterized by $^{87}Sr/^{86}Sr$ signatures that are lower than those depicted by the baseline samples, the bioavailable Sr signatures measured in the plant samples and soil extracts then

reflect the admixture of radiogenic Sr derived from siliciclastic components that are present in the alluvial plains.

The relatively low $^{87}Sr/^{86}Sr$ value of 0.70797 we measured for the spring water collected 1.5 Km south-west of Vergina (Table S6.1) might point to a source to be sought in the ophiolitic rocks, or more probable, to the dominance of Sr in the spring water derived from Cretaceous limestones with a typical range of $^{87}Sr/^{86}Sr$ from 0.7072 to 0.7078 (McArthur et al., 2001) that are prevalent in the Pieria Mountains. In any case, this spring is distant from ancient Vergina and it is almost certain that it was not the source of water for the people at the site. We have therefore excluded this water from the baseline definition for Vergina. An ancient plumbing system was discovered that brought water from a source just above the archaeological site; however, we were not able to locate this spring despite our efforts.

The Pella baseline samples exhibit remarkably homogenous strontium isotope signatures with $^{87}Sr/^{86}Sr$ values ranging from 0.7089 to 0.7091 (Table S6.1). This baseline therefore can be discriminated from that of Vergina ($^{87}Sr/^{86}Sr$ = 0.70996 to 0.70992, potentially broadened to as low as 0.70935; see below). Pella is presently situated in the center of the Thermaikos graben. To the south lie the alluvial plains of the Axios and Aliakmon rivers; to the north lie low hills of Miocene-Pliocene sedimentary rocks deposited long ago in the graben by predecessors of the present rivers. These have been lifted up tectonically and then eroded by the present rivers. It appears, from the signature measured in the undisturbed archaeological soil extract from the Pella excavation (Table S6.1), that the Miocene-Pliocene sedimentary rocks around Pella are characterized by a bioavailable Sr fraction with a $^{87}Sr/^{86}Sr$ value of around 0.7091, a value which is stereotypical of many flysch terranes in central and northern Europe.

Animal tooth enamel and animal bone fragment samples found in Tomb I were also considered for the characterization of the baseline around Vergina. They date a couple of centuries later than the human adult bones.

Table S6.1. Strontium isotope signatures of all the samples analyzed in the framework of this study, complemented by Sr concentrations of a few bone samples.

Sample	Material	$^{87}Sr/^{86}Sr$	+/- ppm	+/- 2σ abs	[Sr] ppm
Pella Baseline					
Sample 1	water from ancient well	0.708974	16	0.000011	
Sample 2	water from ancient well	0.708950	15	0.000011	
Sample 3	water from ancient well	0.708955	10	0.000007	
Sample 4	soil extract from undisturbed archaeological soil	0.709083	9	0.000006	
Vergina Baseline					
Sample 1	oak tree leaves	0.709922	10	0.000007	
Sample 2	leaves from bush	0.709863	7	0.000005	
Sample 3	soil extract from undisturbed archaeological soil	0.709921	9	0.000006	
Sample 4 (excluded from baseline)	spring water (1.5 Km from the site)	0.707974	12	0.000008	
Animal bones from TOMB-1 (included in baseline)					
DEM-3257	*Capra/ovis* tooth enamel	0.709572	11	0.000008	
DEM-3257	*Capra/ovis* maxilla bone	0.709505	10	0.000007	
DEM-3258	*Leporidae* Hare/rabbit, leg bone	0.709350	12	0.000009	
Human samples from TOMB-1					
DEM-3255	Left PM-1 enamel (Mandible-A, male)	0.711353	11	0.000008	
DEM 3256	Left PM-2 enamel (Maxilla-A, male)	0.711676	11	0.000008	
DEM 3237	Left M-1 enamel (Maxilla-B, female)	0.709311	6	0.000004	
DEM-3242	Femur, male	0.708959	25	0.000018	113.8
DEM-3243	Tibia, Male	0.709285	29	0.000021	124.5
DEM-3236	Petrous bone-Left, Male	0.709714	19	0.000013	76.0
DEN-3246	Petrous bone-Right, Female	0.708936	20	0.000014	83.2
DEM-3247	Petrous bone-Left, Female?	0.708570	26	0.000018	116.6

S7. FIGURES AND LEGENDS

S3. Osteological and Odontological Observations

(Photos of bones taken by L. Wynn-Antikas)

Figure S3.1. Left: Right-humerus incomplete (DEM-3239). Right: Left-humerus intact, anterior view proximal ends up.

Figure S3.2. Close up of distal articular ends of the two humeri showing the same morphology and dimensions. Anterior view.

Figure S3.3. The in-situ femora. A) The right femur incomplete (DEM-3242) and B) The left femur complete. Anterior views, proximal ends to the right.

Figure S3.4. Left femur head with the persistence of an epiphyseal line, arrows.

Figure S3.5. In-situ tibiae and fibulae. A: Left tibia (DEM-3243) and fibula (anterior views). B: Right tibia (anterior views) and fibula (medial view) (DEM-3413).

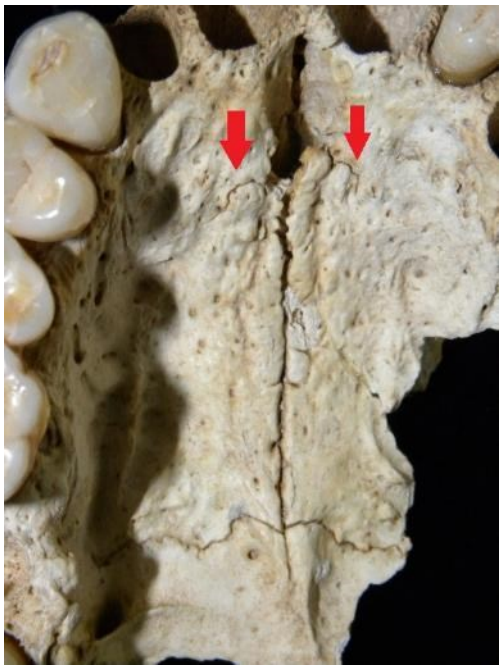

Figure S3.6. Maxilla B (DEM-3237) (The female). The incisive sutures are still in the process of fusing, arrows, inferior view.

Figure S3.7. Left: Right Zygomatic/frontal bone (DEM-3244). Right: Enlargement of the right supra-orbital area. Arrows indicate the rounded supra-orbital margin, typically seen in male morphology (anterior view).

Figure S3.8. Left temporal bone fragment with a long and prominent mastoid process (arrow), typically seen in male morphology.

Figure S3.9. Left: Left ulna (lateral view). Right: Left radius (DEM-3248) (posterior view).

Figure S3.10. A) Right radius (DEM-3125) found in three fragments and B) right intact ulna (anterior view).

Figure S3.11. Right pelvic fragment (DEM-3412), greater sciatic notch.

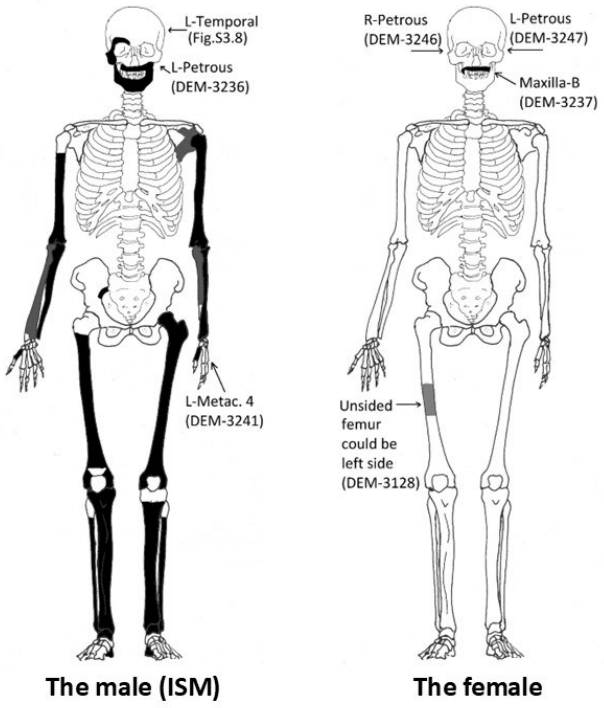

Figure S3.12. Skeleton diagrams showing the bones identified. Left: The In-situ male (ISM) individual. Black: bones found "on the floor", Grey: bones found "in the fill" of the tomb. Refer to Figure 5 and 6 (main manuscript) for the in-situ leg and foot bones on the floor. Additional bones that could not be represented on this diagram but belong to the ISM are: 1) Unsided proximal hand phalange-1 (DEM-3238). 2) Unsided proximal hand phalange-5 (DEM-3134). Right: The Female individual, showing the four bones identified as female.

Figure S3.13. The fused femur and tibia at the Archaeological Museum of Komotini. Recently broken at the joint (Fig. S3.14), but originally fused together at an angle of 79^{o} as shown in the photo. (Photo by Y. Maniatis)

Figure S3.14. The fused femur and tibia separately and a close up of the hole in the tibia, arrow. (Photos by L. Wynn-Antikas)

Figure S3.15. Photo of the Tomb I bones at the Laboratory of Anthropology of the Democritus University of Thrace in 2012. Taken by M. Koutsoumanis, Head of Department of Classical Antiquities and Museums of the Rodopi Ephorate of Antiquities, Komotini. The date of the newspapers is 1985. The arrow indicates the fused pair, neither wrapped in newspaper, nor in tissue and plastic bag, unlike all the other Tomb I bones.

S4. Radiocarbon dating

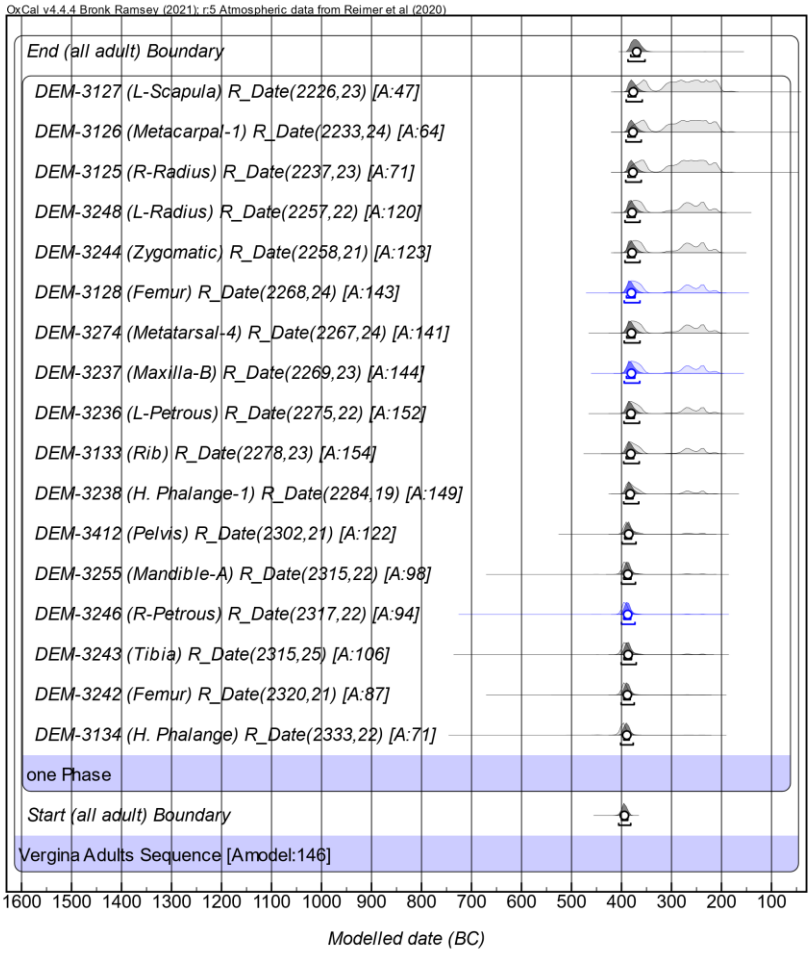

Figure S4.1 (Also, Fig. 12 main manuscript). All adult bones from Tomb I (male, female, "on the floor" and "in the fill"). Bayesian statistical analysis with one-phase model, combined with a general outlier model. Black=male, Blue=female. The open dots indicate the weighted mean value. Plot produced with the program OxCal v.4.4.4 (Bronk Ramsey, 2021).

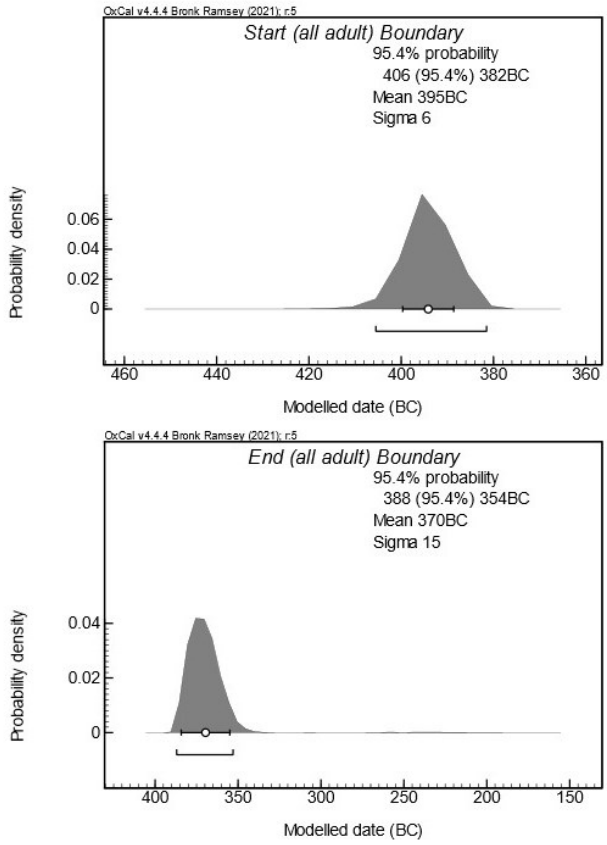

Figure S4.2. Start and End boundaries from the one phase analysis model of all the Tomb I bones (Fig. S4.1). The open dots indicate the weighted mean value. Plots produced with the program OxCal v.4.4.4 (Bronk Ramsey, 2021)

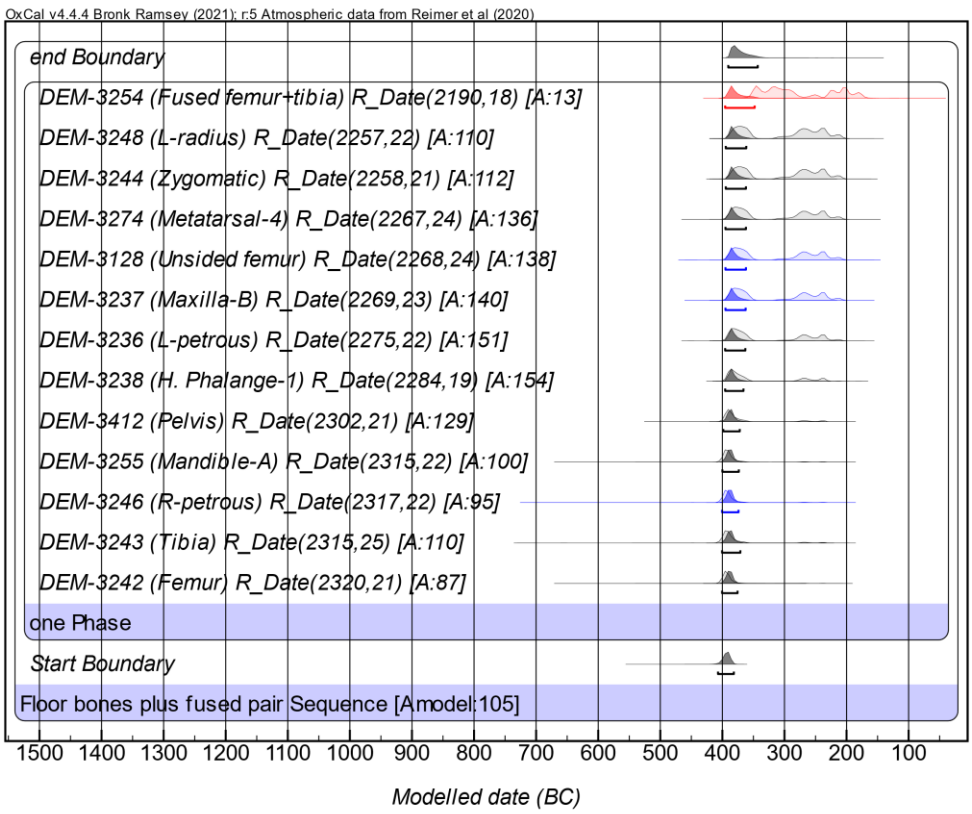

Figure S4.3. The bones "on the floor" (male and female) from Tomb I, plus the fused femur/tibia pair at Komotini. Bayesian statistical analysis with one-phase model, combined with a general outlier model. Black=male, Blue=female, red=the fused femur/tibia pair. Note the extremely low agreement (A:13) of the fused pair compared with the Tomb I floor bones. Plot produced with the program OxCal v.4.4.4 (Bronk Ramsey, 2021).

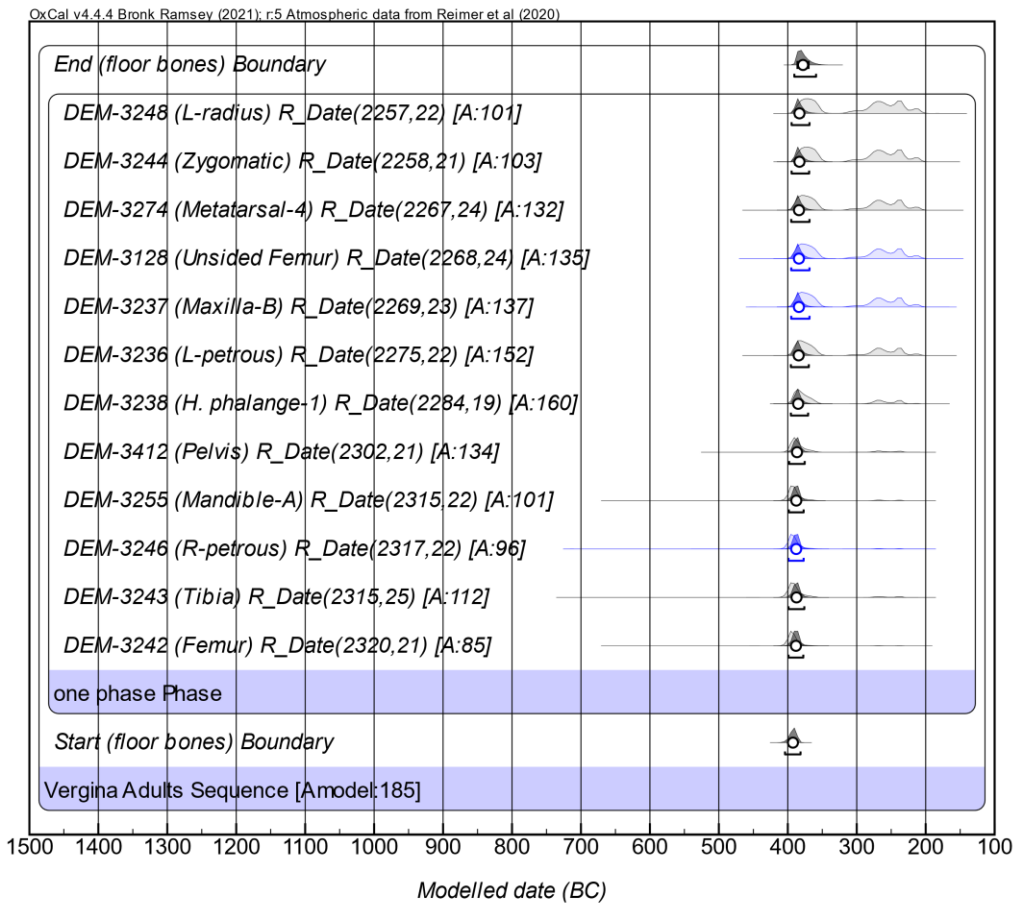

Figure S4.4 (Also, Fig. 13 main manuscript). The bones "on the floor" (male and female) from Tomb I, after removing the fused femur/tibia pair at Komotini. Bayesian statistical analysis with one-phase model, combined with a general outlier model. Black=male, Blue=female, red=the fused femur/tibia pair. Plot produced with the program OxCal v.4.4.4 (Bronk Ramsey, 2021).

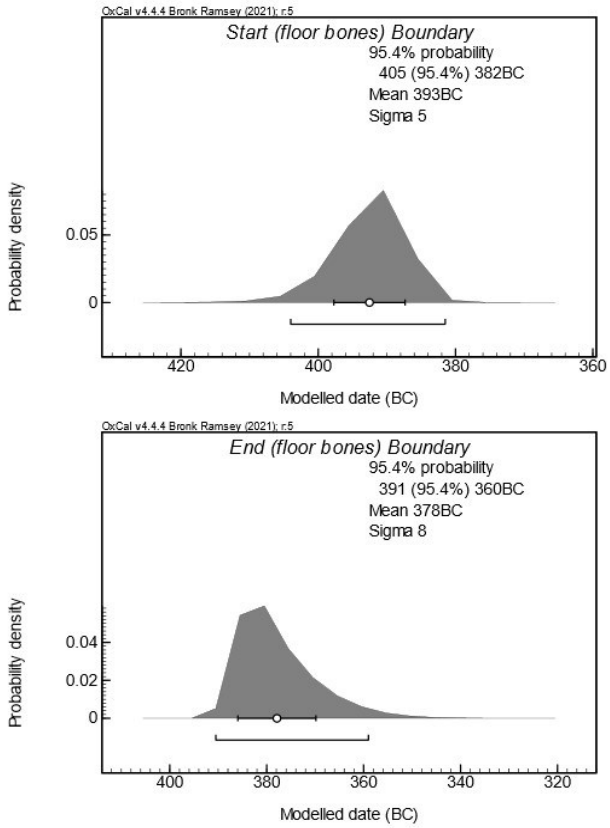

Figure S4.5. Start and End boundaries of the "on the floor" bones from the Bayesian statistical analysis with one-phase model, combined with a general outlier model (Fig. S4.4 and Fig. 13, main manuscript). Plots produced with the program OxCal v.4.4.4 (Bronk Ramsey, 2021).

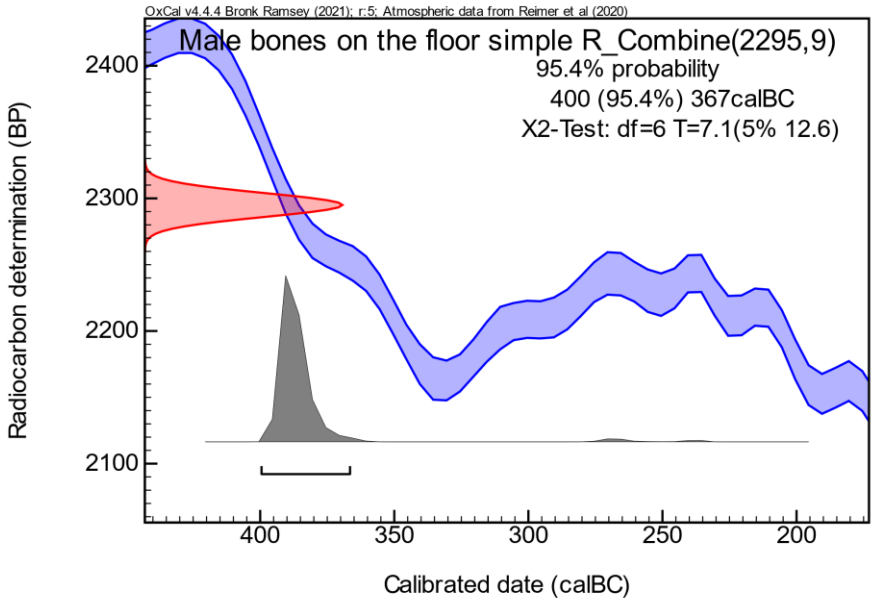

Figure S4.6. R_Combine test for the all the male "on the floor" bones. Plot produced with the program OxCal v.4.4.4 (Bronk Ramsey, 2021).

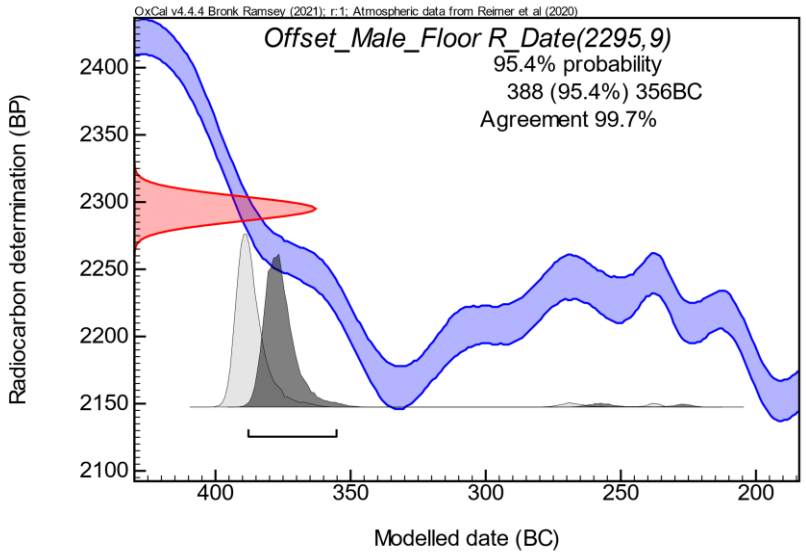

Figure S4.7. Collagen offset correction for all the male "on the floor" bones. Plot produced with the program OxCal v.4.4.4 (Bronk Ramsey, 2021).

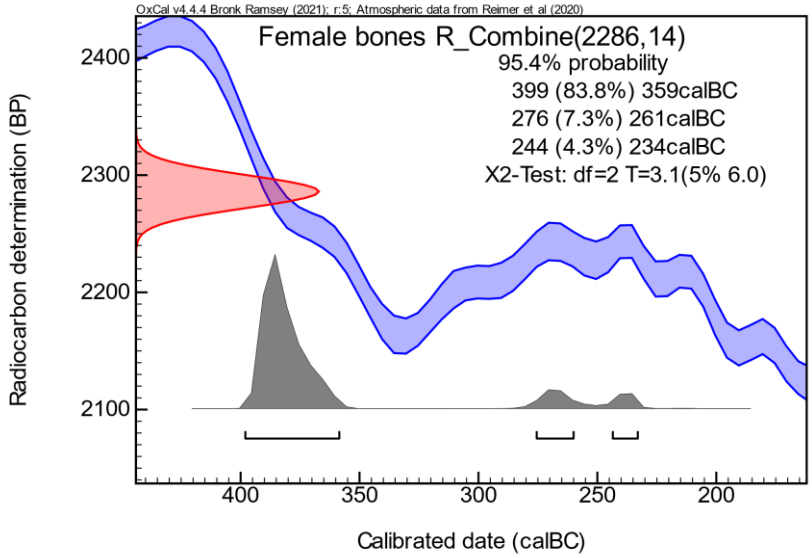

Figure S4.8. R_combine test of the three female bones (DEM-3237, 3246, 3128). Plot produced with the program OxCal v.4.4.4 (Bronk Ramsey, 2021).

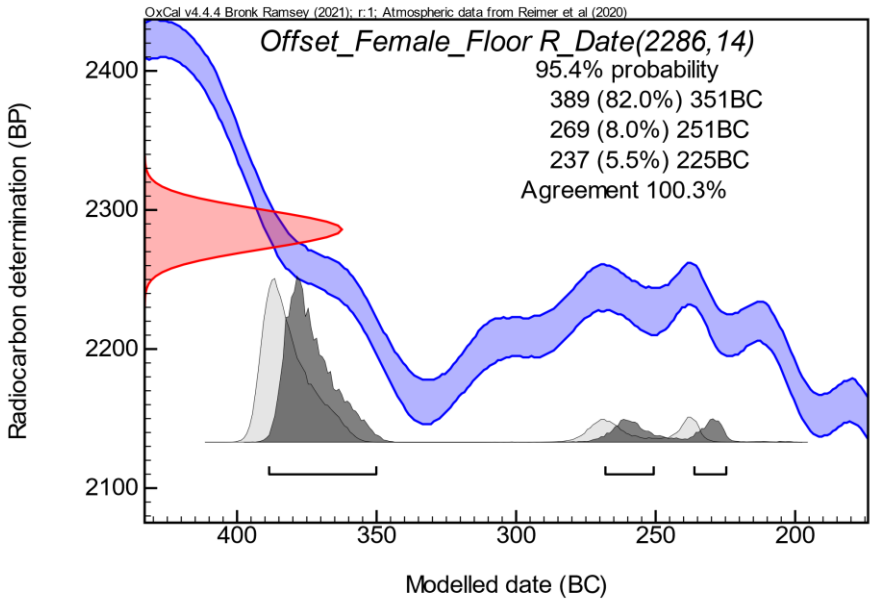

Figure S4.9. Collagen offset correction for all female floor bones. Plot produced with the program OxCal v.4.4.4 (Bronk Ramsey, 2021).

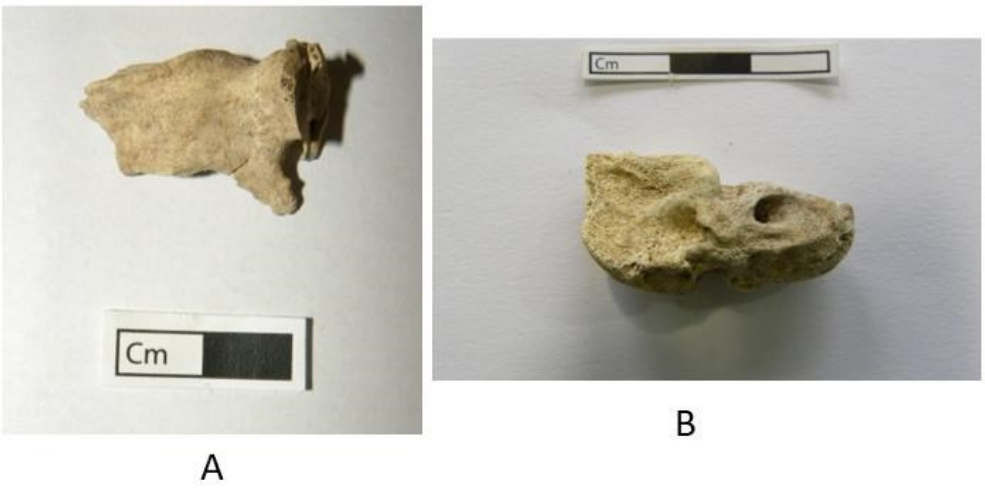

Figure S4.10. Fetus/Perinate bones among the collection of the bones "on the floor" sent to the Archaeological Museum of Thessaloniki and then to Komotini. A: Sphenoid fragment (DEM-3273), B: left petrous bone (DEM-3245). Shown also by Bartsiokas et al (2015, p.35, photo S20).

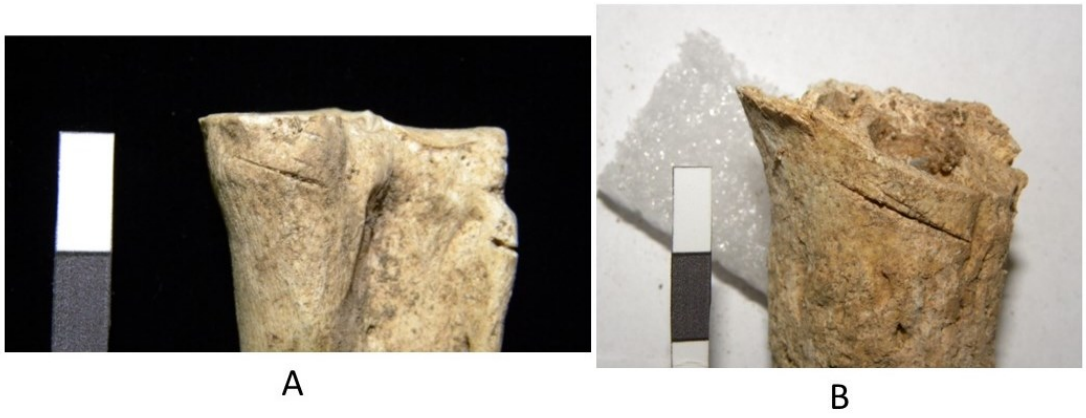

Figure S4.11. Animal bones with butchery marks. A: *Capra/ovis* tibia/fibula bones (DEM-3137), B: *Capra/ovis* horn (DEM-3139).

Figure S4.12. Animal bones and charcoal found north of Tomb I and east of Tomb II. Most probably from a sacrificial pyre over the tombs.

S8. Bibliography

Adams, W.L., 1980. The royal Macedonian tomb of Vergina. An Historical Interpretation. The ancient World 3, 1980, 67-72. The Ancient World 3, 67–72.

Aldossary, M., Alayan, I., Santini, A., 2018. Tooth wear charts as rapid humans age-group assessment methods: A review. International Journal of Information Research and Review 5, 5035–5038.

Ambrose, S.H., 1990. Preparation and characterization of bone and tooth collagen for isotopic analysis. Journal of Archaeological Science 17, 431–451. https://doi.org/10.1016/0305-4403(90)90007-R

Andronikos, M., 1984. Vergina: the royal tombs and the ancient city. Ekdotike Athenon, Athens.

Antikas, T.G., Wynn-Antikas, L.K., 2016. New Finds from the Cremains in Tomb II at Aegae Point to Philip II and a Scythian Princess. Int. J. Osteoarchaeol. 26, 682–692. https://doi.org/10.1002/oa.2459

Apostolidou, C., Eleminiadis, I., Koletsa, T., Natsis, K., Dalampiras, S., Psaroulis, D., Apostolidis, S., Psifidis, A., Tsikaras, P., Njau, S.N., 2011. Application of the Maxillary Suture Obliteration Method For Estimating Age at Death in Greek Population. The Open Forensic Science Journal 4, 15–19. https://doi.org/10.2174/1874402801104010015

Bartsiokas, A., 2000. The Eye Injury of King Philip II and the Skeletal Evidence from the Royal Tomb II at Vergina. Science 288, 511–514.

Bartsiokas, A., Arsuaga, J.L., Brandmeir, N., 2023. The identification of the Royal Tombs in the Great Tumulus at Vergina, Macedonia, Greece: A comprehensive review. Journal of Archaeological Science: Reports 52, 104279. https://doi.org/10.1016/j.jasrep.2023.104279

Bartsiokas, A., Arsuaga, J.-L., Santos, E., Algaba, M., Gómez-Olivencia, A., 2015. The lameness of King Philip II and Royal Tomb I at Vergina, Macedonia. Proceedings of the National Academy of Sciences 112, 9844–9848. https://doi.org/10.1073/pnas.1510906112

Bartsiokas, A., Carney, E., 2008. The Royal skeletal remains from Tomb I at Vergina. Deltos, Journal of the History of Hellenic Medicine 36, 15–19.

Bass, W.M., 1995. Human Osteology: A Laboratory and Field Manual, (4th). ed, Special Publication No.2. Colombia Mo: Missouri Archaeological Society.

Bayliss, A., Hines, J., Høilund Nielsen, K., McCormac, G., Scull, C., 2013. Anglo-Saxon Graves and Grave Goods of the 6th and 7th Centuries AD: A Chronological Framework, in: Hines, J., Bayliss, A. (Eds.), The Society of Medieval Archaeology Monographs, Book 33.

Belcastro, M.G., Pietrobelli, A., Rastelli, E., Iannuzzi, V., Toselli, S., Mariotti, V., 2019. Variations in epiphyseal fusion and persistence of the epiphyseal line in the appendicular skeleton of two identified modern (19th–20th c.) adult Portuguese and Italian samples. American Journal of Physical Anthropology 169, 448–463. https://doi.org/10.1002/ajpa.23839

Borza, E.N., 1987. The Royal Macedonian Tombs and the Paraphernalia of Alexander the Great. Phoenix 41, 105–121. https://doi.org/10.2307/1088739

Borza, E.N., Palagia, O., 2007. The Chronology of the Macedonian Royal Tombs at Vergina. Jahrbuch des Deutschen Archäologischen Instituts 122, 81–125.

Bronk Ramsey, C., 2021. Oxcal v4.4.4 calibration program.

Bronk Ramsey, C., 2009. Dealing with Outliers and Offsets in Radiocarbon Dating. Radiocarbon 51, 1023–1045. https://doi.org/10.1017/S0033822200034093

Brothwell, D.R., 1981. Digging up bones: the excavation, treatment, and study of human skeletal remains, Third. ed. Cornell University Press, Ithaca, New York.

Caduff, M., Eckel, R., Leuenberger, C., Wegmann, D., 2024. Accurate Bayesian inference of sex chromosome karyotypes and sex-linked scaffolds from low-depth sequencing data. Molecular Ecology Resources 24, e13913. https://doi.org/10.1111/1755-0998.13913

Carøe, C., Gopalakrishnan, S., Vinner, L., Mak, S.S.T., Sinding, M.H.S., Samaniego, J.A., Wales, N., Sicheritz-Pontén, T., Gilbert, M.T.P., 2018. Single-tube library preparation for degraded DNA. Methods in Ecology and Evolution 9, 410–419. https://doi.org/10.1111/2041-210X.12871

Cheung, C., Schroeder, H., Hedges, R.E.M., 2012. Diet, social differentiation and cultural change in Roman Britain: new isotopic evidence from Gloucestershire. Archaeological and Anthropological Sciences 4, 61–73. https://doi.org/10.1007/s12520-011-0083-y

Damgaard, P.B., Margaryan, A., Schroeder, H., Orlando, L., Willerslev, E., Allentoft, M.E., 2015. Improving access to endogenous DNA in ancient bones and teeth. Scientific Reports 5, 11184. https://doi.org/10.1038/srep11184

DeNiro, M.J., 1985. Postmortem preservation and alteration of in vivo bone collagen isotope ratios in relation to palaeodietary reconstruction. Nature 317, 806–809. https://doi.org/10.1038/317806a0

Faklaris, P.B., 1994. Aegae: Determining the Site of the First Capital of the Macedonians. American Journal of Archaeology 98, 609–616. https://doi.org/10.2307/506548

Fellows Yates, J.A., Lamnidis, T.C., Borry, M., Andrades Valtueña, A., Fagernäs, Z., Clayton, S., Garcia, M.U., Neukamm, J., Peltzer, A., 2021. Reproducible, portable, and efficient ancient genome reconstruction with nf-core/eager. PeerJ 9, e10947. https://doi.org/10.7717/peerj.10947

Frei, K.M., Mannering, U., Kristiansen, K., Allentoft, M.E., Wilson, A.S., Skals, I., Tridico, S., Nosch, M.-L., Willerslev, E., Clarke, L., Frei, R., 2015. Tracing the dynamic life story of a Bronze Age Female. Scientific Reports 5:10431, 1–7. https://doi.org/10.1038/srep10431

Frei, K.M., Villa, C., Jørkov, M.L., Allentoft, M.E., Kaul, F., Ethelberg, P., Reiter, S.S., Wilson, A.S., Taube, M., Olsen, J., Lynnerup, N., Willerslev, E., Kristiansen, K., Frei, R., 2017. A matter of months: High precision migration chronology of a Bronze Age female. PLoS One 12, e0178834. https://doi.org/10.1371/journal.pone.0178834

Gill, D.W.J., 2008. Inscribed Silver Plate from Tomb II at Vergina: Chronological Implications. Hesperia: The Journal of the American School of Classical Studies at Athens 77, 335–358.

González Fortes, G., Paijmans, J.L.A., 2019. Whole-Genome Capture of Ancient DNA Using Homemade Baits, in: Shapiro, B., Barlow, A., Heintzman, P., Hofreiter, M., Paijmans, J., Soares, A. (Eds.), Ancient DNA. Methods in Molecular Biology. Humana Press, New York, NY.

Grant, D., 2019. Unearthing the Family of Alexander the Great, the Remarkable Discovery of the Royal Tombs of Macedon. Pen and Sword History Press, Yorkshire-Philadelphia.

Green, P., 1982. The Royal Tombs of Vergina: a Historical Analysis, in Adams and Borza 1982, ., in: Adams, W.L., Borza, E.N. (Eds.), Philip II, Alexander the Great and the Macedonian Heritage. Washigton, pp. 129–151.

Hall, J.M., 2014. The Tombs at Vergina, in: Artifact and Artifice.Classical Archaeology and the Ancient Historian. The University of Chicago Press, Chigago and London, pp. 97–117.

Hammond, N.G.L., 1991. The Royal Tombs at Vergina: Evolution and Identities. The Annual of the British School at Athens 86, 69–82.

Hammond, N.G.L., 1982. The Evidence for the Identity of the Royal Tombs at Vergina, in: Adams, W.L., Borza, E.N. (Eds.), Philip II, Alexander the Great and the Macedonian Heritage. Washington, pp. 111–127.

Harbeck, M., Grupe, G., 2009. Experimental chemical degradation compared to natural diagenetic alteration of collagen: implications for collagen quality indicators for stable isotope analysis. Archaeological and Anthropological Sciences 1, 43–57. https://doi.org/10.1007/s12520-009-0004-5

Hatzopoulos, M.B., 2008. The Burial of the Dead (at Vergina) or the Unending Controversy on the Identity of the Occupants of Tomb II. Tekmiria, Centre of Greek and Roman Antiquity, National Foundation of Scientific Research 9, 91–118.

Hedges, R.E.M., Clement, J.G., Thomas, C.D.L., O'Connell, T.C., 2007. Collagen turnover in the adult femoral mid-shaft: Modeled from anthropogenic radiocarbon tracer measurements. American Journal of Physical Anthropology 133, 808–816. https://doi.org/10.1002/ajpa.20598

Hoogewerff, J.A., Reimann, Clemens, Ueckermann, H., Frei, R., Frei, K.M., van Aswegen, T., Stirling, C., Reid, M., Clayton, A., Ladenberger, A., Albanese, S., Andersson, M., Baritz, R., Batista, M.J., Bel-lan, A., Birke, M., Cicchella, D., Demetriades, A., De Vivo, B., De Vos, W., Dinelli, E., Ďuriš, M., Dusza-Dobek, A., Eggen, O.A., Eklund, M., Ernstsen, V., Filzmoser, P., Flight, D.M.A., Forrester, S., Fuchs, M., Fügedi, U., Gilucis, A., Gregorauskiene, V., De Groot, W., Gulan, A., Halamić, J., Haslinger, E., Hayoz, P., Hoffmann, R., Hrvatovic, H., Husnjak, S., Janik, L., Jordan, G., Kaminari, M., Kirby, J., Kivisilla, J., Klos, V., Krone, F., Kwećko, F., Kuti, L., Lima, A., Locutura, J., Lucivjansky, D.P., Mann, A., Mackovych, D., Matschullat, J., McLaughlin, M., Malyuk, B.I., Maquil, R., Meuli, R.G., Mol, G., Negrel, P., Connor, O., Oorts, R.K., Ottesen, R.T., Pasieczna, A., Petersell, W., Pfleiderer, S.., Poňavič, M., Pramuka, S., Prazeres, C., Rauch, U., Radusinović, S., Reimann, C., Sadeghi, M., Salpeteur, I., Scanlon, R., Schedl, A., Scheib, A.J., Schoeters, I., Šefčik, P., Sellersjö, E., Skopljak, F., Slaninka, I., Soriano-Disla, J.M., Šorša, A., Srvkota, R., Stafilov, T., Tarvainen, T., Trendavilov, V., Valera, P., Verougstraete, V., Vidojević, D., Zissimos, A., Zomeni, Z., 2019. Bioavailable 87Sr/86Sr in European soils: A baseline for provenancing studies. Science of The Total Environment 672, 1033–1044. https://doi.org/10.1016/j.scitotenv.2019.03.387

Huang, Y., Ringbauer, H., 2022. hapCon: estimating contamination of ancient genomes by copying from reference haplotypes. Bioinformatics 38, 3768–3777. https://doi.org/10.1093/bioinformatics/btac390

Janko, R., 2018. Papyri from the Great Tumulus at Vergina, Macedonia. Zeitschrift für Papyrologie und Epigraphik 205, 195–206.

Kapp, J.D., Green, R.E., Shapiro, B., 2021. A Fast and Efficient Single-stranded Genomic Library Preparation Method Optimized for Ancient DNA. Journal of Heredity 112, 241–249. https://doi.org/10.1093/jhered/esab012

Kircher, M., Sawyer, S., Meyer, M., 2012. Double indexing overcomes inaccuracies in multiplex sequencing on the Illumina platform. Nucleic Acids Research 40, e3–e3. https://doi.org/10.1093/nar/gkr771

Kottaridi, A., 2020. The Custom of Cremation and the Macedonians. Thoughts on the Finds from the Necropolis of Aigai, in: Macedonian Fragments. Ephorate of Antiquities of Imathia, pp. 89–234.

Kromer, B., Lindauer, S., Synal, H.-A., Wacker, L., 2013. MAMS – A new AMS facility at the Curt-Engelhorn-Centre for Achaeometry, Mannheim, Germany. Nuclear Instruments and Methods in Physics Research Section B: Beam Interactions with Materials and Atoms 294, 11–13. https://doi.org/10.1016/j.nimb.2012.01.015

Lamnidis, T.C., Majander, K., Jeong, C., Salmela, E., Wessman, A., Moiseyev, V., Khartanovich, V., Balanovsky, O., Ongyerth, M., Weihmann, A., Sajantila, A., Kelso, J., Pääbo, S., Onkamo, P., Haak, W., Krause, J., Schiffels, S., 2018. Ancient Fennoscandian genomes reveal origin and spread of Siberian ancestry in Europe. Nature Communications 9, 5018. https://doi.org/10.1038/s41467-018-07483-5

Lane Fox, R.J., 1980. The Search for Alexander. Little, Brown.
Lehmann, P.W., 1980. The So-Called Tomb of Philip II: A Different Interpretation. American Journal of Archaeology 84, 527–531. https://doi.org/10.2307/504082
Levesque, C.G., 2017. The Royal Tombs at Vergina (Honours Thesis). University of New Brunswick, New Brunswick, Canada.
Li, H., Durbin, R., 2009. Fast and accurate short read alignment with Burrows–Wheeler transform. Bioinformatics 25, 1754–1760. https://doi.org/10.1093/bioinformatics/btp324
Li, H., Handsaker, B., Wysoker, A., Fennell, T., Ruan, J., Homer, N., Marth, G., Abecasis, G., Durbin, R., 1000 Genome Project Data Processing Subgroup, 2009. The Sequence Alignment/Map format and SAMtools. Bioinformatics 25, 2078–2079. https://doi.org/10.1093/bioinformatics/btp352
Lovejoy, C.O., 1985. Dental wear in the Libben population: Its functional pattern and role in the determination of adult skeletal age at death. American Journal of Physical Anthropology 68, 47–56. https://doi.org/10.1002/ajpa.1330680105
Mann, R.W., Jantz, R.L., Bass, W.M., Willey, P.S., 1991. Maxillary suture obliteration: a visual method for estimating skeletal age. J Forensic Sci 36, 781–791.
Mann, R.W., Symes, S.A., Bass, W.M., 1987. Maxillary suture obliteration: aging the human skeleton based on intact or fragmentary maxilla. J Forensic Sci 32, 148–157.
Manolagas, S.C., 2000. Birth and Death of Bone Cells: Basic Regulatory Mechanisms and Implications for the Pathogenesis and Treatment of Osteoporosis*. Endocrine Reviews 21, 115–137. https://doi.org/10.1210/edrv.21.2.0395
McArthur, J.M., Howarth, R.J., Bailey, T.R., 2001. Strontium Isotope Stratigraphy: LOWESS Version 3: Best Fit to the Marine Sr-Isotope Curve for 0–509 Ma and Accompanying Look-up Table for Deriving Numerical Age. The Journal of Geology 109, 155–170. https://doi.org/10.1086/319243
Meyer, M., Kircher, M., 2010. Illumina Sequencing Library Preparation for Highly Multiplexed Target Capture and Sequencing. Cold Spring Harbor Protocols 2010, pdb.prot5448. https://doi.org/10.1101/pdb.prot5448
Miles, A.E.W., 1962. Assessment of the Ages of a Population of Anglo-Saxons from Their Dentitions. Proceedings of the Royal Society of Medicine 55, 881–886. https://doi.org/10.1177/003591576205501019
Mincer, H., Harris, E., Berryman, H., 1993. The A.B.F.O. Study of Third Molar Development and Its Use as an Estimator of Chronological Age. Journal of Forensic Sciences 38, 379–390. https://doi.org/10.1520/JFS13418J
Murphy, T., 1959. The changing pattern of dentine exposure in human tooth attrition. American Journal of Physical Anthropology 17, 167–178. https://doi.org/10.1002/ajpa.1330170302
Musgrave, J., Prag, A.J.N.W., Neave, R., Fox, R.L., White, H., 2010. The Occupants of Tomb II at Vergina. Why Arrhidaios and Eurydice must be excluded. Int J Med Sci 7, s1–s15. https://doi.org/10.7150/ijms.7.s1
Musgrave, J.H., 1991. The Human Remains from Vergina Tombs I, II and III: An overview. Ancient World 21, 3–9.
Musgrave, J.H., 1985. The Skull of Philip II of Macedon, in: Lisney, S.J.W., Matthews, B. (Eds.), Current Topics in Oral Biology, Proceedings of a Meeting Held in the Department of Physiology, The Medical School, University of Bristol, UK, on 4 and 5 July 1985 to Mark the Retirement of Professor Declan J. Anderson, Professor of Oral Biology, University of Bristol. pp. 1–16.
Musgrave, J.H., 1984. Some notes on the human remains from Tombs I, II and III at Vergina (Report sent to Professor M. Andronikos and Dr. Vokotopoulou).

Neukamm, J., Peltzer, A., Nieselt, K., 2021. DamageProfiler: fast damage pattern calculation for ancient DNA. Bioinformatics 37, 3652–3653. https://doi.org/10.1093/bioinformatics/btab190

Palagia, O., 2017. The Royal Court in Ancient Macedonia: The Evidence for Royal Tombs, in: The Hellenistic Court: Monarchic Power and Elite Society from Alexander to Cleopatra. Classical Press of Wales, London, pp. 409–431. https://doi.org/10.2307/j.ctt1z27gr0

Philippas, G.G., 1952. Effects of Function on Healthy Teeth: The Evidence of Ancient Athenian Remains. The Journal of the American Dental Association 45, 443–453. https://doi.org/10.14219/jada.archive.1952.0205

Prag, A.J.N.W., 1990. Reconstructing the Skull of Philip of Macedon, in: Danien, E.C. (Ed.), The World of Philip and Alexander: A Symposium on Greek Life and Times. Philadelphia, pp. 35–36.

Quinlan, A.R., Hall, I.M., 2010. BEDTools: a flexible suite of utilities for comparing genomic features. Bioinformatics 26, 841–842. https://doi.org/10.1093/bioinformatics/btq033

Riginos, A.S., 1994. The wounding of Philip II of Macedon: fact and fabrication. Journal of Hellenic studies 114, 103–119.

Rohland, N, Hofreiter, M., 2007. Comparison and optimization of ancient DNA extraction. Biotechniques. 2007;42(3):343-352. doi:10.2144/000112383. Biotechniques 42, 343–352.

Rohland, Nadin, Hofreiter, M., 2007. Ancient DNA extraction from bones and teeth. Nature Protocols 2, 1756–1762. https://doi.org/10.1038/nprot.2007.247

Rohland, N., Siedel, H., Hofreiter, M., 2010. A rapid column-based ancient DNA extraction method for increased sample throughput. Molecular Ecology Resources 10, 677–683. https://doi.org/10.1111/j.1755-0998.2009.02824.x

Saatsoglou-Paliadeli, C., 2011. The royal presence in the Agora of Aegae, in: Galanakis, Y. (Ed.), Heracles to Alexander the Great. Treasures from the Royal Capital of Macedon, a Hellenic Kingdom in the Age of Democracy. Ashmolean Museum, University of Oxford, Oxford, pp. 193–203.

Safont, S., Malgosa, A., Subirà, M.E., 2000. Sex assessment on the basis of long bone circumference. Am J Phys Anthropol 113, 317–328. https://doi.org/10.1002/1096-8644(200011)113:3<317::AID-AJPA4>3.0.CO;2-J

Schubert, M., Ginolhac, A., Lindgreen, S., Thompson, J.F., AL-Rasheid, K.A., Willerslev, E., Krogh, A., Orlando, L., 2012. Improving ancient DNA read mapping against modern reference genomes. BMC Genomics 13, 178. https://doi.org/10.1186/1471-2164-13-178

Schubert, M., Lindgreen, S., Orlando, L., 2016. AdapterRemoval v2: rapid adapter trimming, identification, and read merging. BMC Research Notes 9, 88. https://doi.org/10.1186/s13104-016-1900-2

Sillen, A., 1989. Diagenesis of the inorganic phase of cortical bone, in: Price, T.D. (Ed.), The Chemistry of Prehistoric Human Bone. Cambridge University Press, Cambridge, UK, pp. 211–229.

Sillen, A., 1986. Biogenic and diagenetic Sr/Ca in Plio-Pleistocene fossils of the Omo Shungura Formation. Paleobiology 12, 311–323. https://doi.org/10.1017/S0094837300013816

Skoglund, P., Storå, J., Götherström, A., Jakobsson, M., 2013. Accurate sex identification of ancient human remains using DNA shotgun sequencing. Journal of Archaeological Science 40, 4477–4482. https://doi.org/10.1016/j.jas.2013.07.004

Stewart, T.D., 1979. Essentials of Forensic Anthropology: Especially as Developed in the United States. Charles C. Thomas, Springfield, Illinois.

Surabian, D., 2012. Preservation of Buried Human Remains in Soil. US Department of Agriculture, Natural Resources Conservation Science, Tolland, Connecticut.
Talamo, S., Fewlass, H., Maria, R., Jaouen, K., 2021. “Here we go again”: the inspection of collagen extraction protocols for 14C dating and palaeodietary analysis. STAR: Science & Technology of Archaeological Research 7, 62–77. https://doi.org/10.1080/20548923.2021.1944479
Talamo, S., Richards, M., 2011. A Comparison of Bone Pretreatment Methods for AMS Dating of Samples >30,000 BP. Radiocarbon 53, 443–449. https://doi.org/10.1017/S0033822200034573
Thirlwall, M.F., 1991. Long-term reproducibility of multicollector Sr and Nd isotope ratio analysis. Chemical Geology: Isotope Geoscience section 94, 85–104. https://doi.org/10.1016/0168-9622(91)90002-E
Trotter, M., Gleser, G.C., 1952. Estimation of stature from long bones of American Whites and Negroes. American Journal of Physical Anthropology 10, 463–514. https://doi.org/10.1002/ajpa.1330100407
van Klinken, G.J., 1999. Bone Collagen Quality Indicators for Palaeodietary and Radiocarbon Measurements. Journal of Archaeological Science 26, 687–695. https://doi.org/10.1006/jasc.1998.0385
Xirotiris, N., 2015. Interview with Professor N Xirotiris. The controversy over the tomb of Philip brings revelations (In Greek). Η διαμάχη για τον τάφο του Φιλίππου φέρνει αποκαλύψεις (Article by Mirtsioti Giota).
Xirotiris, N.I., Langenscheidt, F., 1981. The Cremations from the Royal Macedonian Tombs of Vergina. Archaiologiki Ephemeris 142–160.